Comparison of dynamic CT and stable xenon CT in ischemic cerebrovascular disease.

H Touho, J Karasawa, H Ohnishi, K Yamada, K Shibamoto and S Ueda

AJNR Am J Neuroradiol 1993, 14 (3) 655-660
http://www.ajnr.org/content/14/3/655

Comparison of Dynamic CT and Stable Xenon CT in Ischemic Cerebrovascular Disease

Hajime Touho,[1] Jun Karasawa,[1] Hideyuki Ohnishi,[1] Keisuke Yamada,[1] Keiji Shibamoto,[1] and Satoshi Ueda[2]

PURPOSE: To investigate a new hemodynamic parameter that can be obtained by dynamic CT and that reflects cerebral blood flow (CBF), in patients with ischemic cerebrovascular disease. **METHODS:** CBF and hemodynamic parameters including the area under the time-dependent contrast-medium dilution curve (A) and mean transit time (MTT) were measured in 23 patients with ischemic cerebrovascular disease. They included 17 patients in the chronic stage (more than 1 month after onset) and six with acute occlusion of the internal carotid or middle cerebral artery (within 24 hours of onset). CBF measurement was conducted by inhalation of stable xenon during CT scan and the hemodynamic study was performed using dynamic CT. **RESULTS:** CBF in the territory of the middle cerebral artery had an inverse correlation with MTT. (A) divided by (MTT) defined as (f) had a significantly positive correlation with CBF ($MTT = 18.66 - 0.495 \cdot CBF + 0.005 \cdot CBF^2$, $r = .730$, $P < .001$). **CONCLUSION:** This parameter (f) is thought to represent a relative CBF and it can be used in evaluation of the hemodynamic status in ischemic cerebrovascular disease.

Index terms: Brain, ischemia; Xenon, cerebral blood flow; Computed tomography, comparative studies; Efficacy studies

AJNR 14:655–660, May/Jun 1993

Calculation of blood volume from an indicator dilution curve was introduced by Stewart, and was developed and applied chiefly by Hamilton and his group (1–4). The so-called classical Stewart-Hamilton method has recently been validated formally by Meier and Zierler (5, 6). Recent advances in computed tomography (CT) have made it possible to measure local hemodynamics by assessing the flow of contrast material through an organ with rapid-sequence CT scanning immediately after the administration of a bolus of contrast medium (7–9). Dynamic CT can provide considerable information about various organs and it can be applied to intracranial lesions, especially to ischemic cerebrovascular disease (10). In this article, we propose a new hemodynamic parameter that reflects cerebral blood flow (CBF), and discuss its validity and clinical application in patients with ischemic cerebrovascular disease.

Received November 19, 1991; accepted after revisions August 18, 1992.

[1] Department of Neurosurgery, Osaka Neurological Institute, 2-6-23 Shonai-Takara-machi, Toyonoaka, Osaka, 561, Japan. Address reprint requests to Hajime Touho, MD.

[2] Department of Neurosurgery, Kyoto Prefectural University of Medicine, 465 Kajii-cho, Hirokoji, Kawara-machi, Kamigyo-ku, Kyoto, Japan.

AJNR 14:655–660, May/Jun 1993 0195-6108/93/1403–0655

Materials and Methods

Between January 1, 1990 and September 30, 1990, 23 patients with ischemic cerebrovascular disease were admitted to our institution. They included 17 patients in the chronic stage (more than 1 month after onset) and six in the acute stage (within 24 hours of onset) with stenosis or occlusion of the internal carotid or middle cerebral artery. The former group included eight patients with severe stenosis or occlusion of the internal carotid artery and nine with severe stenosis or occlusion of the middle cerebral artery. Just after their admission, measurement of CBF with the inhalation of stable xenon (Xe^s) and CT scanning (Quantex RX, Yokogawa Medical Systems, Tokyo, Japan) plus dynamic CT were performed following plain CT scanning.

CBF Measurement

A flat rubber face mask was designed to ensure a tight fit for all patients. Throughout the measurement process, the electrocardiogram, spontaneous carbon dioxide gas concentrations, and spontaneous Xe^s gas concentrations in both inspiratory and expiratory phases were measured

continuously. The Xe^s gas concentrations were measured with a thermoconductivity gas analyzer.

After two control scans, 30% Xe^s mixed with oxygen was inhaled for 240 seconds (wash-in phase) followed by a washout phase of 160 seconds to desaturate Xe^s. To decrease the total volume of Xe^s gas, a cold xenon gas delivery system (AZ-723, Anzai Sogyo, Tokyo, Japan) was used. A CT scanner with a 512 × 512 matrix and 10-mm collimation (Quantex RX, Yokogawa Medical Systems) was used in this study. Exposure factors included a 3-second scanning time, 120 kVp, and 130 mA, which are thought to minimize the standard deviations with the scanner data. Although the smoothing process reduces the resolution of the functional image, we performed it because the concentration of Xe^s used was as low as 30% and the inhalation time as short as 4 minutes.

During wash-in and washout phases, 10 serial CT scans were obtained every 20 seconds for each scan level for CBF analysis. End tidal Xe^s gas concentrations were continuously monitored and recorded and the arterial build-up rate constant (K) and build-up range (A) were calculated on-line according to the following equations:

$$ha(t) = Aa[e^{-Ka(t-\tau)} - e^{-Kat}] \quad (A)$$

$$hi(t) = Ai[g(t - \tau) - g(t)] \quad (B)$$

where

$$[e^{-Kit} + Ki(e^{-kit} - e^{-Kat})/(Ka - Ki)]$$

is replaced by

$$g(t)Ai = \lambda i \cdot Aa \quad (C)$$

and $\tau = t$ for $0 < t < T$, and $\tau = T$ for $t > T$, ha(t), hi(t) are the increases in Hounsfield units for Xe^s gas, respectively. Ka and Ki are the build-up rate constants and Aa and Ai are the build-up ranges for artery and cerebral tissue, respectively. λi is defined as the partition coefficient for brain tissue and T is the duration of inhalation of Xe^s gas. ha(t) shows a linear exponential increase and decrease and hi(t) then shows a biexponential increase and decrease. Aa, Ka, Ai, and Ki were calculated from the time-dependent Xe^s concentrations in the arterial blood and cerebral tissue of interest, by the least-squares method applied to the above equations.

$$Ea = [ha(Tm) - Aa(e^{-Kat(Tm-\tau)} - e^{KaTm})]^2 \quad (D)$$

$$Ei = \{hi(Tm) - Ai[g(Tm - \tau) - g(Tm)]\}^2 \quad (E)$$

where ha(Tm) and hi(Tm) are measured values and $Aa(e^{-Ka(Tm-\tau)}-e^{-KaTm})$, and Ai[g(Tm-τ)-g(Tm)] are calculated values fitted by the equations (A) and (B).

The values of λi (=Ai/Aa) and Ki are calculated to minimize the values of both Ea and Ei. Since the inflow time of Xe^s in the brain (Tx) occurs after the start of Xe^s inhalation, Tx is increased from 0 to 10 seconds at 2-second intervals following the start of Xe^s inhalation, and a suitable Tx is selected on-line so minimum values of Ea, Aa and Ka can be calculated in real time.

Finally, $fi = 100 \cdot \lambda i \cdot Ki$ (mL/100 g cerebral tissue/min), where fi is the local cerebral blood flow.

In our model, K and A for artery and cerebral tissue can be calculated simultaneously, as both Ea and Ei become minimum with the least-squares method ($\delta E/\delta A = \delta E/\delta K = 0$) (11, 12).

Dynamic CT

Following CBF measurement, dynamic CT on one selected section was performed with Iopamidol (E.R. Squibb & Sons, Princeton, NJ) (the contrast medium, 300 mg of iodine per milliliter) injected via a 19-gauge Teflon catheter inserted into a brachial vein. The volume of the contrast medium used was 30 mL delivered at a rate of 8 mL/second using an auto-injector. The scanning sequence was a 4-second clockwise scan, followed by a 2-second interscan delay and then a 4-second counterclockwise scan. This sequence was repeated for a total of six scans. CT functional images to give information about the area under the time-dependent CT number curve (A), mean transit time (MTT:center of gravity of the area, as described by Zierler (13)), and relative flow value (defined as the former parameter divided by the latter) were created from the intrinsic data obtained by dynamic CT. The time-dependent data obtained from each 360° scan were separated into three consecutive but overlapping (216°) segments. A gamma variate function was fitted to the curve obtained (14), and hemodynamic maps were then displayed as CT functional images by assigning a shade of gray depending on the value of the parameter selected. Regions of interest for the analysis of CBF and the hemodynamic state were routinely placed in the territories of both middle cerebral arteries (Fig. 1).

The hemodynamic parameters obtained were as follows: 1) CBF; 2) MTT; 3) area (A); 4) (A/MTT) × (k) (=f, k is an arbitrary factor to bring the f value closer to CBF, the value of which is 70); 5) CBF on the left side/CBF on the right

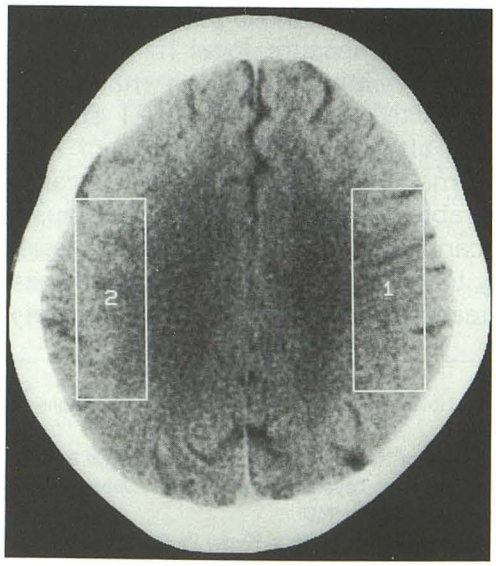

Fig. 1. Regions of interest for the analysis of cerebral blood flow and the hemodynamic state were usually placed in the territories of both middle cerebral arteries (*1* and *2*).

side (%CBF); 6) MTT on the left side/MTT on the right side (%MTT); 7) A on the left side/A on the right side (%A); 8) f on the left side/f on the right side (%f); and 9) MTT × CBF on the left side/MTT × CBF on the right side (%(MTT × CBF), which corresponds to cerebral blood volume).

Results

The correlation between CBF and MTT was investigated in the 23 patients. If cerebral blood volume remains constant, then changes in MTT reflect CBF inversely according to the Stewart-Hamilton formula (MTT = CBV/CBF) (Fig. 2, $MTT = 18.66 - 0.495 \cdot CBF + 0.005 \cdot CBF^2$, $r = .730$, $P < .001$). As shown in Fig. 3, the %MTT was also inversely correlated with %CBF ($\%MTT = 2.251 - 1.914 \cdot \%CBF + 0.637 \cdot \%CBF^2$, $r = .906$, $P < .001$).

We next investigated the relationship between the parameter f and CBF, and found that f had a significant positive correlation with CBF ($f = 0.69 \times CBF + 3.47$, $n = 46$, $r = .4026$, $P < .01$). In addition, %f also correlated significantly with %CBF (Fig. 4, $\%f = 1.12 \times \%CBF - 0.097$, $n = 23$, $r = .7288$, $P < .001$).

We then investigated whether the (A) represented CBV (MTT × CBF) or not. Figure 5 demonstrates the result, indicating that %A had a significant positive correlation with %(MTT × CBF) ($\%A = 0.65 \times [\%(MTT \times CBF)] + 0.30$, $n = 23$, $r = .4772$, $P < .05$).

Illustrative Case

A 73-year-old man was admitted with left hemiparesis, hemihypesthesia, and dressing apraxia. He had a history of cerebral infarction 3 months before admission. CT scans demonstrated a small low-density area in the right basal ganglia (Fig. 6, left). Cerebral angiograms showed occlusion of the right internal carotid artery with collateral flow via the ipsilateral ophthalmic artery (Fig. 7). The proximal segment of the left anterior cerebral artery (A_1) was hypoplastic. Xe^s-CT demonstrated a moderately low flow area in the territories of the right internal carotid and left anterior cerebral arteries (Fig. 8, middle), and dynamic CT showed a moderate increase in the value of A and a moderately prolonged MTT in the relevant region (Fig. 6, middle and right, respectively). The f map closely resembled the CBF map as showed in Figure 8 (left and middle, respectively) and the f/CBF map showed relatively uniform values in both cerebral hemispheres (Fig. 8, right).

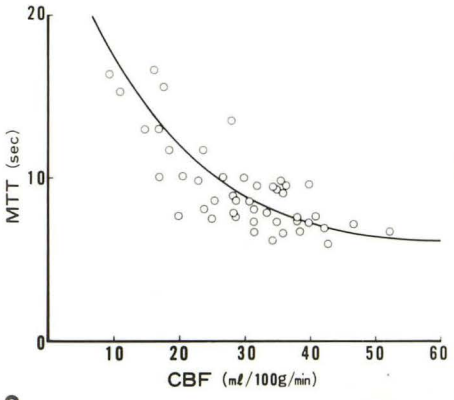

2

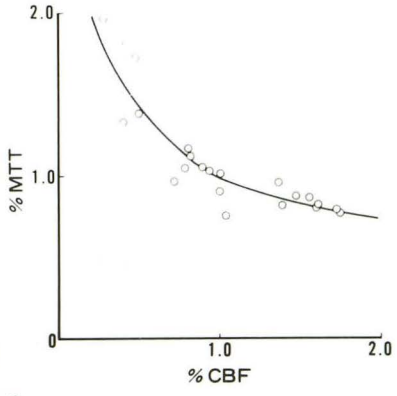

3

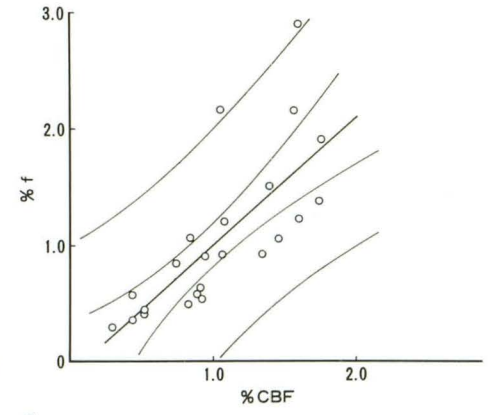

4

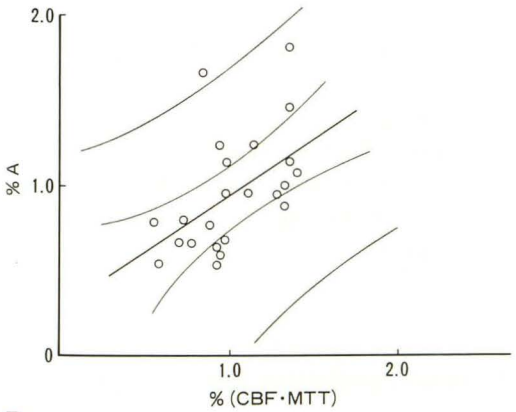

5

Fig. 2. The relationship between cerebral blood flow (*CBF*) and mean transit time (*MTT*) is shown. *MTT* is inversely correlated to *CBF*.

Fig.3. The relationship between *%CBF* and *%MTT* is shown. *%MTT* is inversely correlated to *%CBF*. (*%CBF* and *%MTT* are defined in the text.)

Fig. 4. The relationship between *%CBF* and *%f* is shown. *%f* has a significant positive correlation with *%CBF*. (*%CBF* and *%f* are defined in the text.)

Fig. 5. The relationship between *%(CBF × MTT)* and *%A* is shown. *%A* has a significant positive correlation with *%(CBF × MTT)*. (*%(CBF × MTT)* and *%A* are defined in the text).

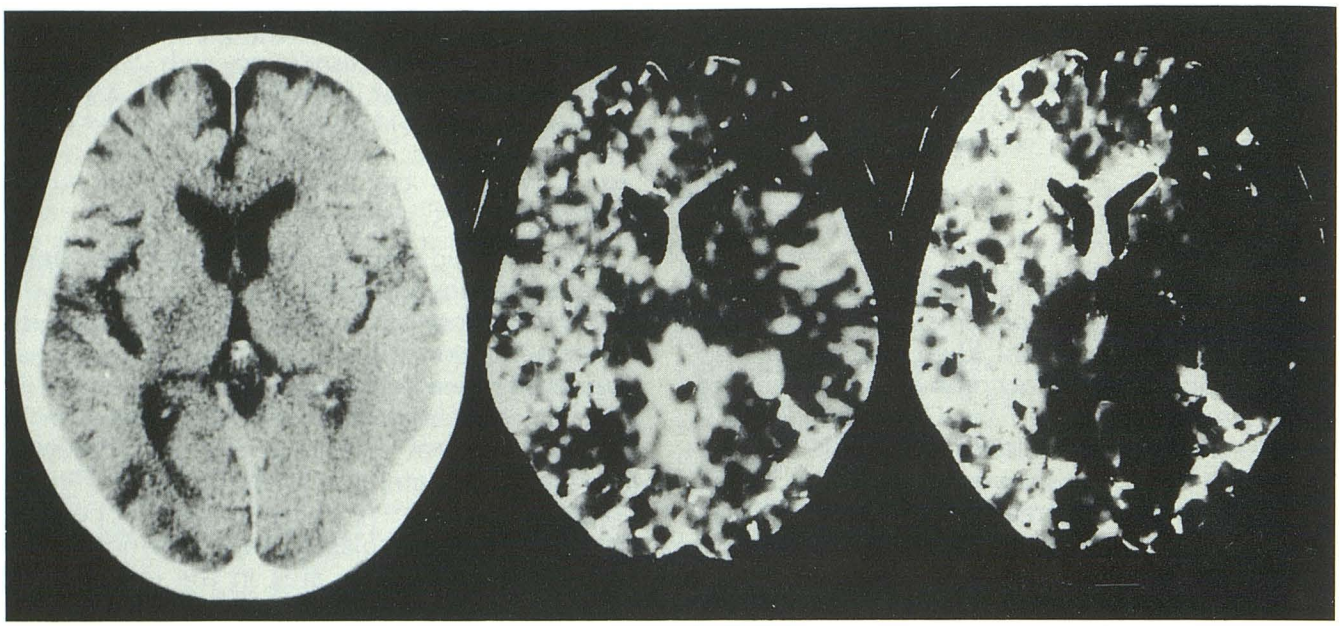

Fig. 6. Plain CT (*left*), area (A) map (*middle*), and MTT map (*right*) in a 73-year-old man with occlusion of the right internal carotid artery are shown. There is a low-density area in the right basal ganglia on plain CT. The values of (A) in the territories of the right internal carotid artery and of the left anterior cerebral artery are markedly increased compared to those in the left hemisphere, and MTT is prolonged in the relevant area with increased (A).

Discussion

The intracranial circulation time can be measured using a nondiffusible indicator according to Stewart's method (14, 15). Various methods for measurement of the transit time have been described.

One method is the direct inspection of serial angiograms and angiodensitometry of the regional cerebral circulation. With serial angiography, it is possible to obtain an indicator dilution curve for various areas in the brain and the T1/2 is calculated for the descending limb (washout process) by plotting the indicator quantity on a semilogarithmic graph (16–19). Measurement of the transit time using an intravenous injection of radioisotope is also possible. The transit time is defined as the time between the first and second inflection points on a time-dependent radioactivity curve and is called the mode of transit time (20). Measurement of the MTT, defined as $\int tCtdt/\int Ctdt$ (Ct: concentration of indicator at time t), is possible (13). In this study, we applied MTT to determine the local transit time in the brain.

Measurement of cerebral blood volume (CBV) always has been difficult. Several attempts have been made, and some of those methods such as emission CT studies using radioactively labeled erythrocytes described by Kuhl et al have proved useful but they are not widely available (21). To circumvent the problem, the method is used that involves the simultaneous measurement of CBF and MTT of a nondiffusible indicator by rapid sequential scanning after intravenous injection of a bolus of contrast medium. Calculating CBV by multiplying CBF by MTT was first reported in the early 1970s (22, 23). CT scanners have become faster allowing a more accurate estimate of MTT. However, the potential exists for errors in the measurement of blood volume because of variety of input functions and overlapping effect (24). Nevertheless, this method holds promise for evaluation of CBV in various states. Based on previous studies, normal CBV values in humans appear to be between 4 and 5 mL/100 g (21, 25). Bouma et al reported physiologically reasonable CBV values calculated by this method (24).

Axel has described CBF determination by rapid-sequence CT, in which the blood flow per unit of total tissue volume is determined by measuring the concentration of contrast material in the blood. This cannot always be done directly from brain scans, but a relative value for the total tissue flow can be calculated by using the area under the curve of the contrast concentration as a function of time ($\int Ctdt$), because this area is thought to be proportional to the fractional vascular volume of any particular tissue (u) [$u \propto \int Ctdt$ (A value)] (15).

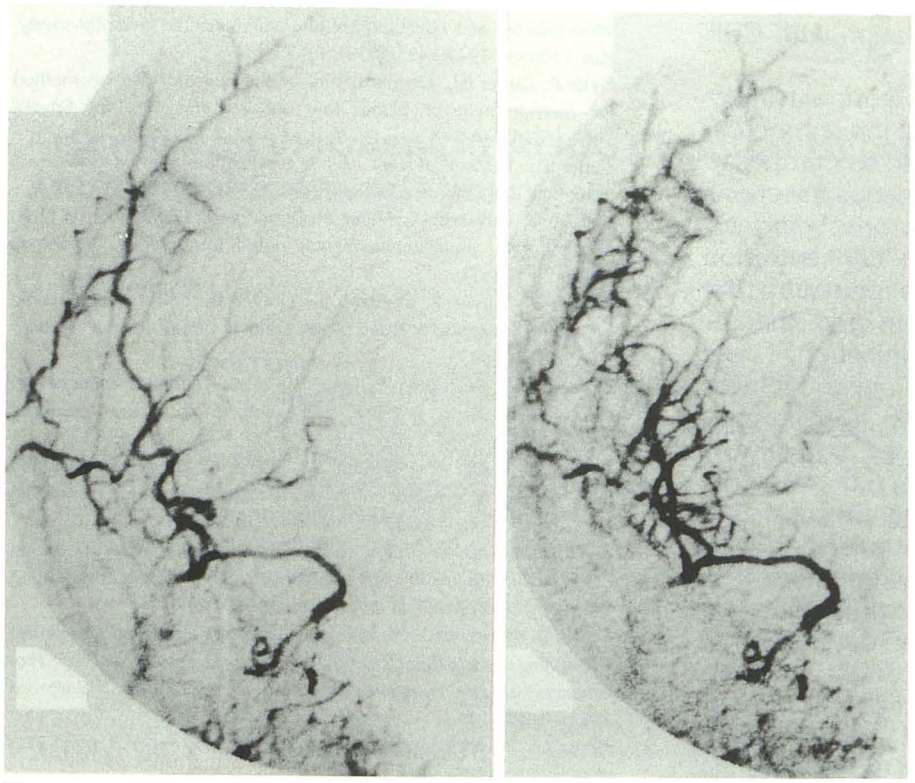

Fig. 7. The right common carotid artery angiograms (anteroposterior view) in the same patient in Figure 6. These angiograms demonstrated occlusion of the right internal carotid artery with collateral via the ipsilateral ophthalmic artery.

7

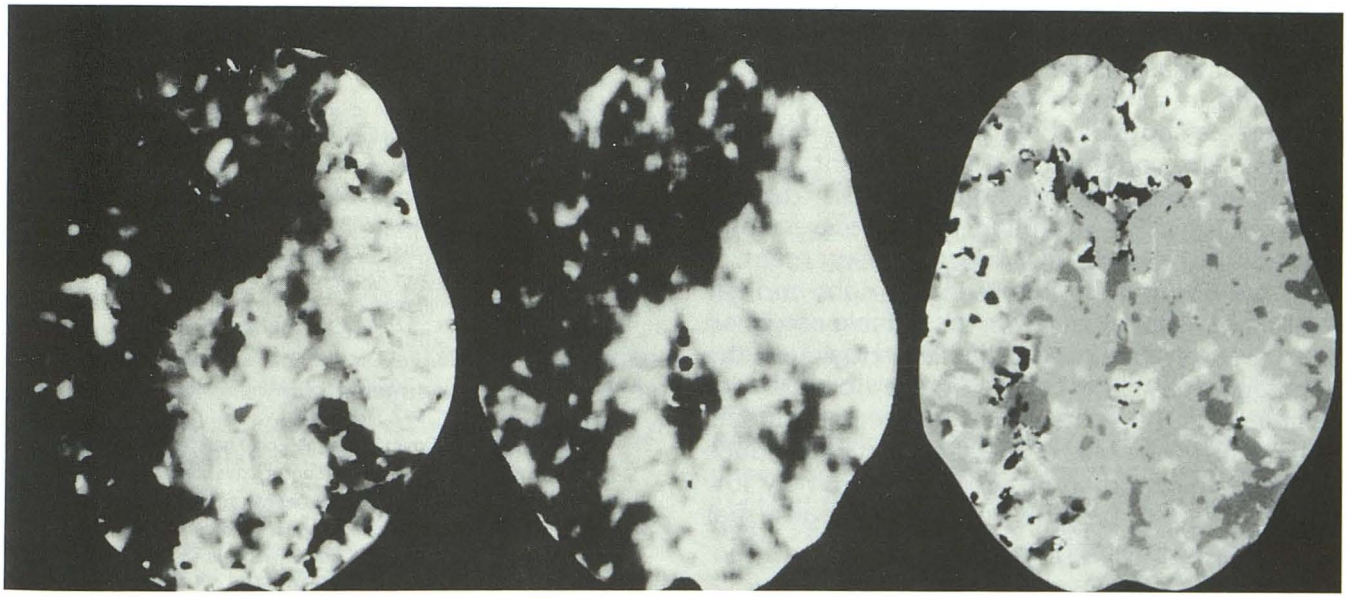

Fig. 8. f map (*left*), CBF map (*middle*), and f/CBF map (*right*) are demonstrated in the same patients in Figure 6. The f map closely resembles the CBF map and the f/CBF map discloses relatively uniform values in both cerebral hemispheres.

According to the classical Stewart-Hamilton method, there must exist some unique time defined as $v = q \times t$ where there is a net volume, v, between the entrance and the exit boundaries and if the flow occurs at a steady rate (q), the time, t, can then be calculated as follows: $t = \int tCtdt / \int Ctdt$.

Therefore, we defined the relative blood flow as A/MTT according to the Stewart-Hamilton formula (blood flow = blood volume/mean transit time), and compared this parameter with CBF as measured by the Xe^s CT method. There was a significant positive correlation between %(A/MTT) and %CBF. Moreover, the A value also

showed significant positive correlation with CBF × MTT, which reflects CBV.

If, instead of an instantaneous contrast injection at time t = 0, a more general input function is visualized, it can be considered to be composed of a continuous series of instantaneous injections with the tissue response to each one being superimposed. The resulting tissue concentration as a function of time would be given by the convolution of the input function and the response to an instantaneous bolus injection. These parameters have to be precisely deconvoluted when the tissue response function is being calculated. However, in this study the convoluted forms of the functions were analyzed and compared with the absolute CBF value. From a clinical viewpoint, A/MTT showed a correlation with CBF. However, one must always remember that the vascular bed volume can be expressed as the area (A) under the curve obtained as a function of time when integration of the input function ($\int$Cadt, where Ca is the arterial concentration of a contrast material) is constant, for example, when stenosis and/or occlusion of an intracranial artery occurs with preservation of cross-flow and/or antegrade flow. In contrast, in the case of stenosis and/or occlusion and functioning leptomeningeal anastomoses, the input function may be altered, resulting in inequality of the two parameters as shown in Figures 4 and 5.

There are some limitations inherent to this technique, because functional images derived from dynamic CT scanning using contrast medium do not permit the direct measurement of CBF, but comparison between the right and left cerebral hemispheres allows the reliable detection of an area of abnormal perfusion. However, the technique may not be applicable to posterior fossa lesions, because spatial frequency artifacts and the intrinsic noise of the scanner can produce incorrect values in some areas of extremely low vascularity and provide for poor images that could lead to misinterpretation.

References

1. Stewart GN. Researchers on the circulation time in organs and on the influences which affect it. Part 1 to Part 2. *J Physiol* 1894;15:1–89
2. Stewart GN. Researchers on the circulation time and on the influences which affect it. Part 4. The output of the heart. *J Physiol* 1898;22:159–183
3. Hamilton WF, Moore JW, Kinsman JM, Spurling RG. Further analysis of the injection method, and of changes in hemodynamics under physiological and pathological. *Am J Physiol* 1932;99:534–551
4. Hamilton WF, Remington JW. Comparison of the time concentration curves in arterial blood of diffusible and nondiffusible substances when injected at a constant rate and when injected instantaneously. *Am J Physiol* 1947;148:35–39
5. Meier P, Zierler KL. On the theory of the indicator-dilution method for measurement of blood flow and volume. *J Appl Physiol* 1954;6:731–744
6. Zierler KL. Theoretical basis of indicator-dilution methods for measuring flow and volume. *Circ Res* 1962;10:393–407
7. Dobben G, Valvassori G, Mafee M, Berninger W. Evaluation of brain circulation by rapid rotational computed tomography. *Radiology* 1979;133:105–111
8. Heinz ER, Dubois P, Osborne D, Drayer B, Barret W. Dynamic computed tomography study of the brain. *J Comput Assist Tomogr* 1979;3:641–649
9. Berninger W, Redington R, Leue W, et al. Technical aspects and clinical applications of CT/X, a dynamic CT scanner. *J Comput Assist Tomogr* 1981;5:206–215
10. Traupe H, Heiss W, Hoeffken W, Zuilch K. Hyperperfusion and enhancement in dynamic computed tomography of ischemic stroke patients. *J Comput Assist Tomogr* 1979;3:627–632
11. Touho H, Karasawa J, Nakagawara J, et al. Mapping of local cerebral blood flow with stable xenon-enhanced CT and the curve-fitting method of analysis. *Radiology* 1988;168:207–212
12. Touho H, Karasawa J. Clinical application of stable xenon-enhanced CT in the management of ischemic cerebrovascular disease. *Proceedings of the Japanese Congress of Neurological Surgeons* 1991;10:120–139
13. Zierler KL. Equations for measuring blood flow by external monitoring of radioisotope. *Circ Res* 1965;16:309–321
14. Thompson H Jr, Starmer CF, Whalen R, McIntosh D. Indicator transit time considered as a gamma variate. *Circ Res*1964;14:502–514
15. Axel L. Cerebral blood flow determination by rapid-sequence computed tomography: a theoretical analysis. *Radiology* 1980;137:679–686
16. Greitz T. Radiologic study of the brain circulation by rapid serial angiography of the carotid artery. *Acta Radiol* 1956; suppl 140
17. Greitz T. Normal cerebral circulation time as determined by carotid angiography with sodium and methylglucamine diatrizoate (Urografin). *Acta Radiol (Diagn) (Stockh)* 1968;7:331–336
18. Hilal SK. Human carotid artery flow determination using a radiographic technique. *Invest Radiol* 1966;1:113–122
19. Moniz E. Sur la vitesse du sang dans l'organism. *Ann Med* 1932;32:193–220
20. Oldendorf WH. Measurement of the mean transit time of cerebral circulation by external detection of an intravenously injected radioisotope. *J Nucl Med* 1962;3:382–398
21. Kuhl D, Alavi A, Hoffman EJ, et al. Local cerebral blood volume in head injured patients: determination of emission computed tomography of ^{99m}Tc-labeled red cells. *J Neurosurg* 1980;52:309–320
22. Smith AL, Neufeld GR, Omnisky AJ, Wollman H. Effect of arterial CO_2 tension on cerebral blood flow, mean transit time, and vascular volume. *J Appl Physiol* 1971;31:701–707
23. Mathew NT, Meyer JS, Bell RL, Johnson PC, Neblett CR. Regional cerebral blood flow and blood volume measured with gamma camera. *Neuroradiology* 1972;4:133–140
24. Bouma GJ, Fatouros PP, Muizelaar JP, et al. Determination of cerebral blood volume by simultaneous xenon-enhanced computed tomographic cerebral blood flow measurement and dynamic comuted tomography enhanced by intravenous contrast. In: Yonas H, ed. *Cerebral blood flow measurement with stable xenon-enhanced computed tomography*. New York: Raven Press, 1992:100–104
25. Grubb RL Jr, Raichle ME, Higgins CS, Eichling JO. Measurement of regional cerebral blood volume by emission tomography. *Ann Neurol* 1978;4:322–328